the plant journal

SEB Society for Experimental Biology

The Plant Journal (2016) **86,** 363–375 doi: 10.1111/tpj.13177

An essential role of caffeoyl shikimate esterase in monolignol biosynthesis in *Medicago truncatula*

Chan Man Ha[1,2], Luis Escamilla-Trevino[1,2,3], Juan Carlos Serrani Yarce[1,2,3], Hoon Kim[4,5], John Ralph[4,5], Fang Chen[1,2,3] and Richard A. Dixon[1,2,3,*]

[1]*BioDiscovery Institute, University of North Texas, Denton, TX 76203, USA,*

[2]*Department of Biological Sciences, University of North Texas, Denton, TX 76203, USA,*

[3]*BioEnergy Science Center (BESC), Oak Ridge National Laboratory, Oak Ridge, TN 37831, USA,*

[4]*Department of Biochemistry, University of Wisconsin, Madison, WI 53726, USA, and*

[5]*US Department of Energy, Great Lakes Bioenergy Research Center (GLBRC), Wisconsin Energy Institute, 1522 University Avenue, Madison, WI 53726, USA*

Received 15 January 2016; revised 21 March 2016; accepted 24 March 2016; published online 2 April 2016.
*For correspondence (e-mail richard.dixon@unt.edu)

SUMMARY

Biochemical and genetic analyses have previously identified caffeoyl shikimate esterase (CSE) as an enzyme in the monolignol biosynthesis pathway in *Arabidopsis thaliana*, although the generality of this finding has been questioned. Here we show the presence of *CSE* genes and associated enzyme activity in barrel medic (*Medicago truncatula*, dicot, Leguminosae), poplar (*Populus deltoides*, dicot, Salicaceae), and switchgrass (*Panicum virgatum*, monocot, Poaceae). Loss of function of CSE in transposon insertion lines of *M. truncatula* results in severe dwarfing, altered development, reduction in lignin content, and preferential accumulation of hydroxyphenyl units in lignin, indicating that the CSE enzyme is critical for normal lignification in this species. However, the model grass *Brachypodium distachyon* and corn (*Zea mays*) do not possess orthologs of the currently characterized CSE genes, and crude protein extracts from stems of these species exhibit only a weak esterase activity with caffeoyl shikimate. Our results suggest that the reaction catalyzed by CSE may not be essential for lignification in all plant species.

Keywords: *Brachypodium distachyon*, esterase, lignin biosynthesis, *Medicago truncatula*, switchgrass.

INTRODUCTION

Lignin is a complex phenylpropanoid-derived polymer that is a major structural component of plant secondary cell walls. Lignin in angiosperms is composed primarily of guaiacyl (G) and syringyl (S) monolignols, with much smaller levels of hydroxyphenyl (H) units. It was proposed over 12 years ago that the reaction responsible for insertion of the hydroxyl group at the 3-position of the *p*-hydroxyphenyl intermediates to produce the G and S monolignols occurs predominantly at the level of the shikimate ester of *p*-coumarate rather than at that of the free acid or its coenzyme A derivative (Humphreys and Chapple, 2002) (Figure 1). This conclusion is supported by the demonstration that the enzyme HCT (hydroxycinnamoyl CoA: shikimate/quinate hydroxycinnamoyl transferase) is involved in lignin biosynthesis based on the strong reductions in lignin accumulation observed upon down-regulation of its activity (Hoffmann *et al.*, 2004; Shadle *et al.*, 2007), and the identification of the enzyme encoded by the gene target of the *ref8* mutation in Arabidopsis as a coumaroyl shikimate 3′-hydroxylase (C3′H) (Franke *et al.*, 2002). For this so-called 'shikimate shunt' to operate in lignin biosynthesis, it is generally postulated that HCT can act in the reverse direction to convert the product of the C3′H reaction, caffeoyl shikimate, to caffeoyl CoA, the substrate for the first methylation enzyme, caffeoyl CoA 3-*O*-methyltransferase (CCoAOMT) in the lignin pathway (Figure 1b). However, the reverse HCT reaction, although measurable *in vitro*, is generally very inefficient (Hoffmann *et al.*, 2004; Escamilla-Treviño *et al.*, 2014; Wang *et al.*, 2014), and cannot be detected in crude extracts from switchgrass (Escamilla-Treviño *et al.*, 2014).

Our understanding of this pathway took a surprising turn in 2013 when it was demonstrated than an enzyme capable of selectively hydrolyzing caffeoyl shikimate to caffeic acid was present in *Arabidopsis thaliana* (Vanholme *et al.*, 2013b). Loss of function of this caffeoyl shikimate

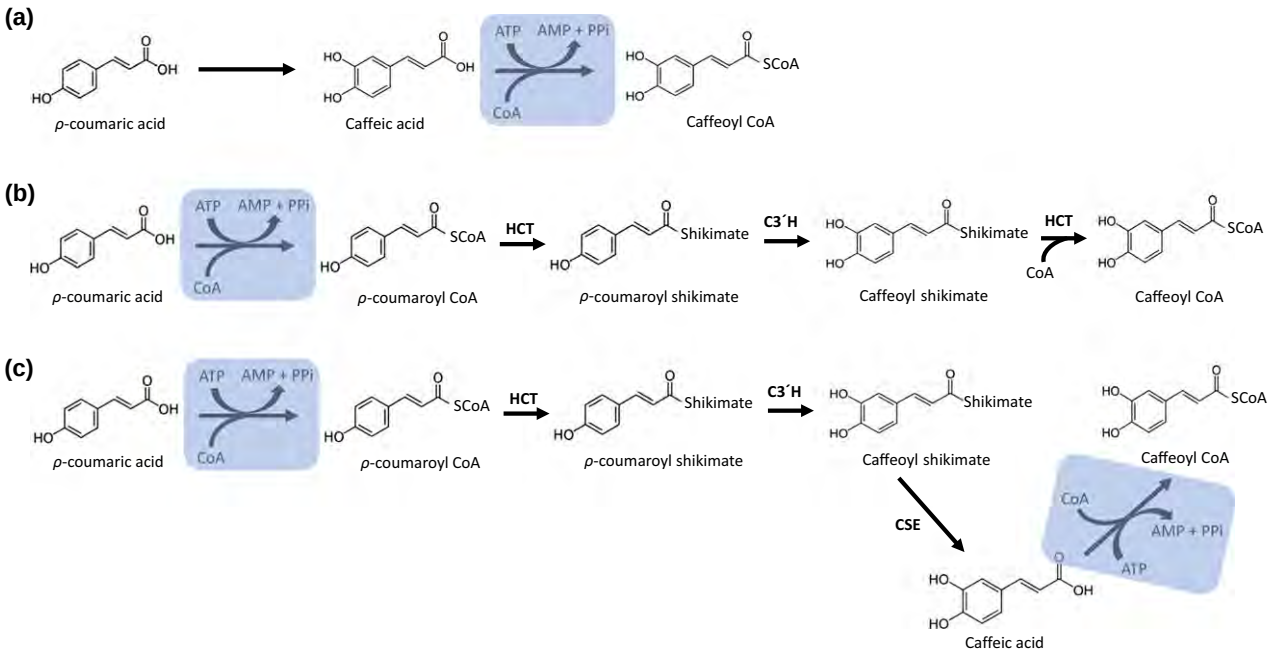

Figure 1. Pathways from coumarate to caffeoyl CoA in monolignol biosynthesis.
(a) Hydroxylation at the level of free acids.
(b,c) The shikimate shunt involving both forward and reverse reactions of HCT (b), and the involvement of CSE (c).
The HCT and C3′H reactions are labelled, and the reactions involving CoA esterification via hydrolysis of ATP are highlighted.

esterase (CSE) in Arabidopsis resulted in reduced lignin levels, an increased fraction of *p*-hydroxyphenyl (H) units in lignin, and a 40% reduction in plant growth (Vanholme *et al.*, 2013b). Although supported by the genetic evidence, the involvement of this enzyme in lignin biosynthesis at first appears counter-intuitive, as it necessitates the consumption of an additional molecule of ATP to re-form the CoA thioester that is then methylated by CCoAOMT (Figure 1b). Note that formation of caffeoyl CoA through the 'reverse' *trans*-esterification reaction of HCT does not consume ATP. Doubts as to the general role of CSE in lignin biosynthesis were then raised in a study in which metabolic flux into lignin in poplar (*Populus trichocarpa*) was modelled based on a combined analysis of the *in vitro* kinetics and inhibition constants of all the enzymes believed, at the time, to be involved in monolignol formation (Wang *et al.*, 2014). Although two CSE homologs are present in the *P. trichocarpa* genome, the authors concluded that CSE need not be considered in their kinetic model, as no CSE activity could be detected in extracts from poplar secondary developing xylem (Wang *et al.*, 2014). The authors also reported that no CSE activity could be detected in extracts from secondary developing xylem of *Eucalyptus grandis*, or from stems of switchgrass (*Panicum virgatum*) or rice (*Oryza sativa*).

To further assess the role of CSE in lignification, we here examine the phylogenetic distribution of the enzyme among monocots and dicots, examine the activity of the enzyme from two dicots (*Populus deltoides* and *Medicago truncatula*) and two monocots (switchgrass and *Brachypodium distachyon*), and investigate the effects of loss of function of CSE in *M. truncatula*. *CSE* genes and corresponding enzyme activities were present in all these species except for *B. distachyon*. CSE appears to be critical for lignin biosynthesis in *M. truncatula*, in which loss of function results in a phenotype that is even more severe than that reported previously in Arabidopsis (Vanholme *et al.*, 2013b).

RESULTS

Phylogenetic analysis of CSE and CSE-like proteins

CSE belongs to the α/β-hydrolase superfamily of proteins. To address CSE function across species, we first carried out phylogenetic analysis of 149 CSE homologous proteins from 61 plant species using the *Arabidopsis thaliana* CSE protein sequence as the query (Figure 2). The proteins largely grouped into two classes. Class I included potentially *bona fide CSE* genes closely related to AtCSE (At1g52760); among these, the *CSE* genes from *A. thaliana*, *M. truncatula* (Medtr4g127220), and rice (*Oryza sativa*) had no additional homologous sequences in their corresponding genomes, whereas the *CSE* genes from poplar (*Populus deltoides* and *P. trichocarpa*) and switchgrass (*Panicum virgatum*) had two additional sequences. Protein sequence alignments of the CSE proteins from *A. thaliana*,

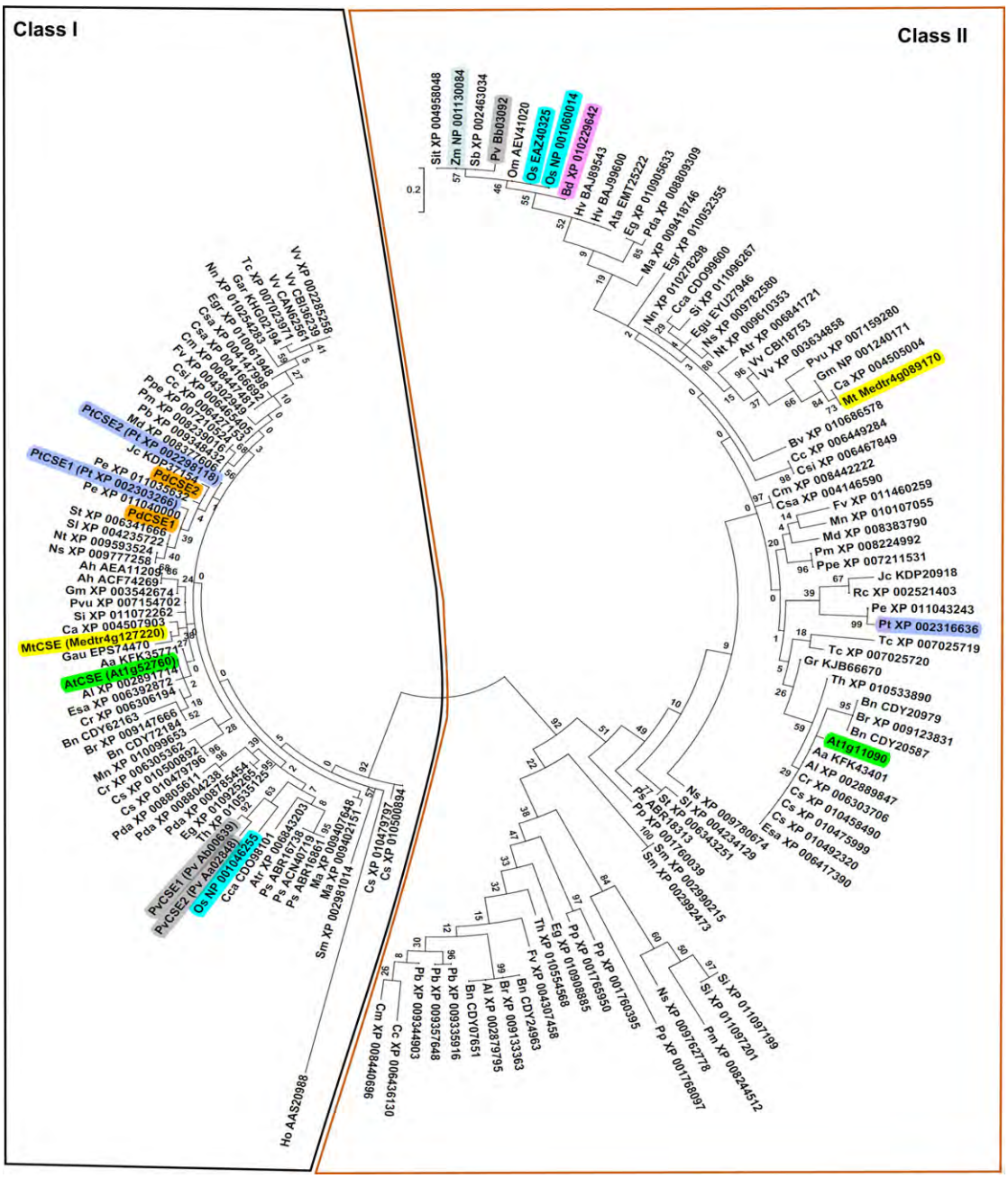

Figure 2. Phylogenetic analysis of *CSE* and *CSE*-like genes from 61 plant species.

The maximum likelihood phylogeny of 149 CSE and CSE-like amino acid sequences. The multiple sequence alignment of these sequences was used to build the phylogeny with 1000 bootstrap analyses. The protein sequence of AtCSE (At1 g52760) was used as a query to BLAST (BLASTP) against the non-redundant protein sequence database of NCBI. Sequences from switchgrass (*Panicum virgatum*) were obtained via Phytozome v10.2. Species are: Aa, *Arabis alpine*; Ata, *Aegilops tauschii*; Ah, *Arachis hypogaea*; Al, *Arabidopsis lyrata* subsp. *Lyrata*; Atr, *Amborella trichopoda*; At, *Arabidopsis thaliana*; Bd, *Brachypodium distachyon*; Bn, *Brassica napus*; Br, *Brassica rapa*; Bv, *Beta vulgaris* subsp. *vulgaris*; Ca, *Cicer arietinum*; Cc, *Citrus clementina*; Cca, *Coffea canephora*; Cm, *Cucumis melo*; Cr, *Capsella rubella*; Cs, *Camelina sativa*; Csa, *Cucumis sativus*; Csi, *Citrus sinensis*; Eg, *Elaeis guineensis*; Egr, *Eucalyptus grandis*; Egu, *Erythranthe guttata*; Esa, *Eutrema salsugineum*; Fv, *Fragaria vesca* subsp. *vesca*; Gar, *Gossypium arboretum*; Gau, *Genlisea aurea*; Gm, *Glycine max*; Gr, *Gossypium raimondii*; Ho, *Hyacinthus orientalis*; Hv, *Hordeum vulgare* subsp. *vulgare*; Jc, *Jatropha curcas*; Ma, *Musa acuminata* subsp. *malaccensis*; Md, *Malus domestica*; Mn, *Morus notabilis*; Mt, *Medicago truncatula*; Nn, *Nelumbo nucifera*; Ns, *Nicotiana sylvestris*; Nt, *Nicotiana tomentosiformis*; Om, *Oryza minuta*; Os, *Oryza sativa* Japonica Group (Japanese rice); Pb, *Pyrus* × *bretschneider*; Pd, *Populus deltoides*; Pda, *Phoenix dactylifera*; Pe, *Populus euphratica*; Pm, *Prunus mume*; Pp, *Physcomitrella patens*; Ppe, *Prunus persica*; Ps, *Picea sitchensis*; Pt, *Populus trichocarpa* (poplar); Pv, *Panicum virgatum* (switchgrass); Pvu, *Phaseolus vulgaris*; Rc, *Ricinus communis*; Sb, *Sorghum bicolor*; Si, *Sesamum indicum*; Sit, *Setaria italic*; Sl, *Solanum lycopersicum*; Sm, *Selaginella moellendorffii*; St, *Solanum tuberosum*; Tc, *Theobroma cacao*; Th, *Tarenaya hassleriana*; Vv, *Vitis vinifera*; Zm, *Zea mays*.

The phylogenetic tree was constructed using MEGA 6 (Tamura *et al.*, 2013) with 1000 bootstrap replicates. Numbers indicate the percentage of consensus support. Plant proteins of interest in *M. truncatula, A. thaliana*, rice, *Brachypodium*, poplar and switchgrass are highlighted.

M. truncatula, *P. deltoides*, *P. trichocarpa* and *P. virgatum* are shown in Figure S1. Class II CSEs included CSE homologs with low sequence identity (below 40% identity in amino acid sequence to the AtCSE protein sequence). Interestingly, CSE homologous sequences from *B. distachyon* and corn (*Zea mays*) were found only in this class. Both classes were represented by genes from all angiosperm lineages including eudicots, monocots and lycopods (e.g. *Selaginella*) and gymnosperm lineages including Pinophyta (e.g. *Picea sitchensis*).

Functional characterization of CSE proteins

We next attempted to confirm the functional activities of proteins encoded by the candidate *CSE* genes from *M. truncatula* and poplar. The open reading frames from the single *M. truncatula CSE* and the two *P. deltoides CSE* genes were expressed in *E. coli* as His-tagged proteins, and the recombinant proteins purified by nickel affinity chromatography and tested for CSE activity by incubation with caffeoyl shikimate using reaction conditions as previously reported (Escamilla-Treviño *et al.*, 2014). When caffeoyl shikimate was incubated in reaction buffer for 4 h in the absence of enzyme, high pressure liquid chromatography (HPLC) analysis revealed a small amount of a new product (peak 2 in Figure 3a), with an identical UV spectrum to that of caffeoyl shikimate (Figure 3j) and a mass spectrum showing the major ion of caffeoyl shikimate (m/z 335.1), but with three additional minor ions of m/z 454.9, 291.0 and 135.0 (Figure S2a,b). Furthermore, the secondary ion of caffeoyl shikimate at m/z 179.0 was of higher intensity. These observations suggest that this compound is an adduct formed between the substrate and components present in the buffer; the compound was not present if the CSE reaction was stopped at zero time by reducing the pH (Figure 3b). Recombinant *M. truncatula* CSE converted caffeoyl shikimate to a single product *in vitro*, with 100% conversion under the reaction conditions used (Figure 3d); the product exhibited identical retention time (Figure 3c), and UV (Figure 3i) and mass (Figure S2c) spectra to a sample of authentic caffeic acid. Caffeic acid was likewise generated by the recombinant CSE from *P. deltoides*, although the sample analyzed in Figure 3(e) did not catalyze complete conversion over the 4 h incubation, and this allowed some of the caffeoyl shikimate adduct to form. The partial conversion may reflect *in vitro* stability of the *P. deltoides* CSE, because a sample that had been stored for less time at −80°C did catalyze complete conversion within 4 h. Both recombinant *P. deltoides* CSEs exhibited similar activity.

CSE activity in switchgrass and two species that lack a class I CSE gene, *B. distachyon* and corn, was analyzed by performing enzyme assays with crude protein extracts from stem tissues. Crude switchgrass extracts gave approximately 50% conversion of caffeoyl shikimate to caffeic acid as the main product, along with the caffeoyl shikimate adduct (Figure 3f). In contrast, equal amounts of crude stem protein from *Brachypodium* and corn produced only very small amounts of caffeic acid, with the adduct being the major product (Figure 3g,h). It is not clear whether the low level formation of caffeic acid reflects the activity of a non-specific esterase, or the activity of a class II CSE homolog, in these species.

Identification of CSE loss-of-function mutants in *M. truncatula*

The above studies clearly confirm the existence of CSE enzyme activity in three plant species. However, because of the low, possibly non-specific, esterase activity in lignifying tissues of *B. distachyon* and corn, the report that the enzyme is not active in lignifying tissues of *P. trichocarpa* (Wang *et al.*, 2014), and the relatively weak phenotype associated with loss of CSE function in *A. thaliana* (Vanholme *et al.*, 2013b) when compared to the loss of function of HCT (the enzyme believed to be responsible for caffeoyl CoA biosynthesis in earlier models of monolignol synthesis) (Li *et al.*, 2010) (Figure 1b), there is need for additional genetic evidence for CSE function. We therefore investigated the involvement of CSE in monolignol biosynthesis through loss-of-function genetic analysis in *M. truncatula*, a species well suited to reverse genetic approaches (Naoumkina *et al.*, 2010; Liu *et al.*, 2014). The *CSE* gene of *M. truncatula* consists of a single exon without intron (Figure 4a), and is strongly expressed in the stem and root, whereas expression is weak in old mature seeds (Figure S3). We screened an *M. truncatula* Tnt1 retrotransposon insertion population (Tadege *et al.*, 2005, 2008) and found two lines with insertion of the retrotransposon in different positions in the exon region of the *CSE* gene. The independent mutant lines (NF13103 and NF17462) were renamed *Mtcse*-1 and *Mtcse*-2, respectively (Figure 4a). There were no *MtCSE* transcripts detected in either mutant allele (Figure 4b).

Growth and developmental phenotypes of *Mtcse* mutants

Mtcse mutant plants showed a severely dwarfed phenotype (Figure 4c). To better document this, we measured plant growth every 4 days over the course of plant development. The stems of the control plants bolted at about 23 days after germination, whereas bolting was delayed in the mutant stems until approximately 43 days after germination (Figure 4d and Table 1). The control plants flowered at about 55 days after germination, whereas flowering was delayed in *Mtcse* mutant plants until about 80 days after germination. In contrast, the Arabidopsis *cse* mutant bolted and flowered at the same time as the control plant (Table 1). The inflorescence stem height of the control plants increased gradually to reach 115 cm at full maturity in 3-month-old plants. In contrast, inflorescence stem growth in the mutants was delayed and the stems reached

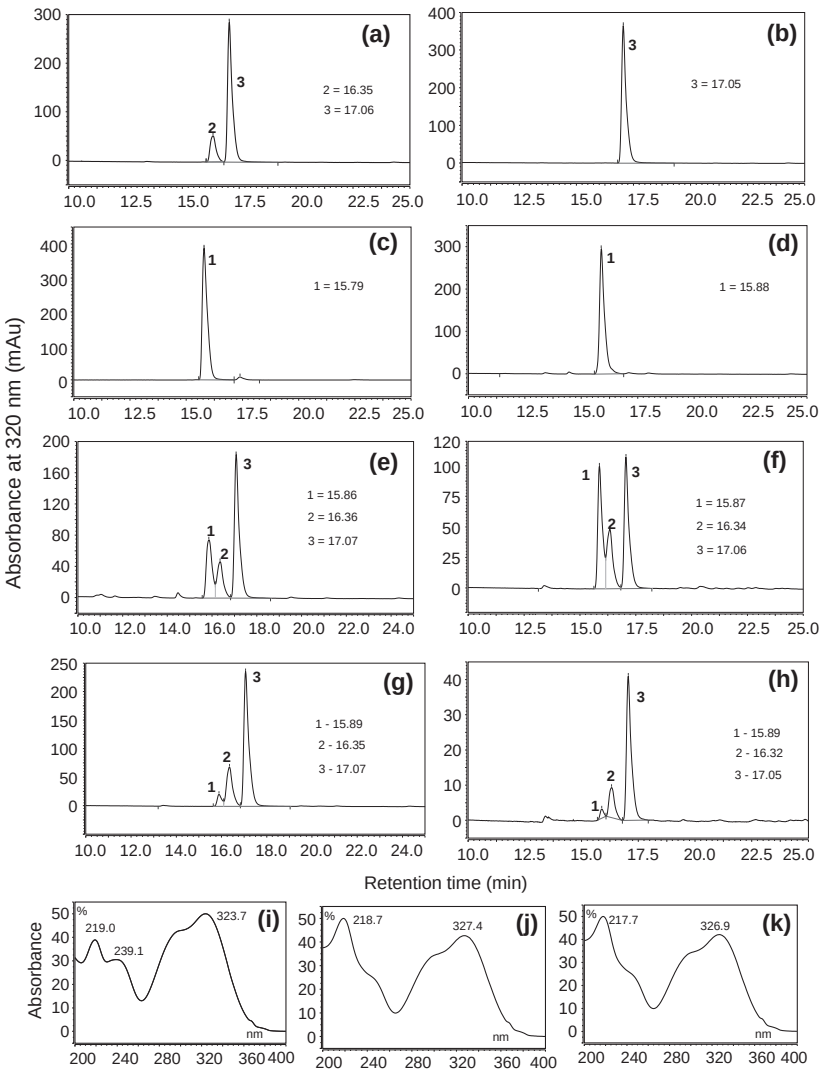

Figure 3. HPLC chromatograms showing products of reactions with recombinant CSE proteins from *P. deltoides* and *M. truncatula* and crude protein extracts from switchgrass, *Brachypodium* and corn. All incubations were for 4 h.
(a) Caffeoyl shikimate standard, incubated in reaction buffer.
(b) Caffeoyl shikimate incubated with switchgrass extract for 4 h, but reaction stopped at $t = 0$.
(c) Caffeic acid standard.
(d) Product from incubation of recombinant MtCSE with caffeoyl shikimate.
(e) Products from incubation of recombinant poplar PdCSE1 with caffeoyl shikimate; the chromatogram obtained with recombinant poplar PdCSE2 showed a similar level of conversion to caffeic acid.
(f) Products from incubation of crude protein preparation from stems of switchgrass with caffeoyl shikimate.
(g) Products from incubation of crude protein preparation from stems of *Brachypodium* with caffeoyl shikimate.
(h) Products from incubation of crude protein preparation from stems of corn with caffeoyl shikimate.
(i) UV spectrum of peak 1 (caffeic acid).
(j) UV spectrum of peak 2 (caffeoyl shikimate adduct).
(k) UV spectrum of peak 3 (caffeoyl shikimate substrate).
Numbers of the peaks refer to retention time in min, indicated on the panels. Mass spectra of peaks 1–3 are given in Figure S2.

only 10 cm when fully grown. *Mtcse* mutant plants also displayed delayed senescence in both leaf and flower development (Figure S4). The seed pods in mutant plants started to develop at 3 months, at which time the seed pods in control plants were already starting to senesce. In addition, the size of the seed pods in mutant plants was much smaller than in control plants (Figure S4b). Furthermore, control plants produced seven or eight seeds per seed pod, whereas mutant plants produced only one or two seeds per pod.

To further characterize *Mtcse* mutant plants, stem cross-sections were observed with UV light, under which lignin- and wall-bound phenolic compounds exhibit blue autofluorescence. Compared with control stems, *Mtcse* mutant stems were thinner (compare Figure 5a,f) and exhibited similar autofluorescence but abnormal morphology (compare Figure 5a–c, f–h), with highly decreased number of vessel elements. Xylem vessel elements in the mutant stems were collapsed (Figure 5h, arrows), implying the development of weakened secondary cell walls (Jones *et al.*, 2001; Thévenin *et al.*, 2011). We next examined stem sections by Wiesner (phloroglucinol) staining, which is considered to reflect lignin content but is somewhat specific for coniferaldehyde end groups in lignins (Lewis and Yamamoto, 1990; Pomar *et al.*, 2002). Interestingly, *Mtcse* mutant plants had strongly increased Wiesner staining of the vascular tissue compared with control stems (compare Figure 5d, i). It is possible that free soluble phenolics (e.g. hydroxycinnamyl aldehydes) might contribute to the dark colour of the mutant stems after Wiesner staining. To test this hypothesis, we removed soluble phenolics by treating stem sections in methanol and chloroform. This procedure had little effect on the appearance of cross-sections from wild-type plants (compare Figure S5a–e and Figure 5a–e). Cross-sections of stems from the *cse* mutant exhibited a brighter yellow appearance of the unstained organ after

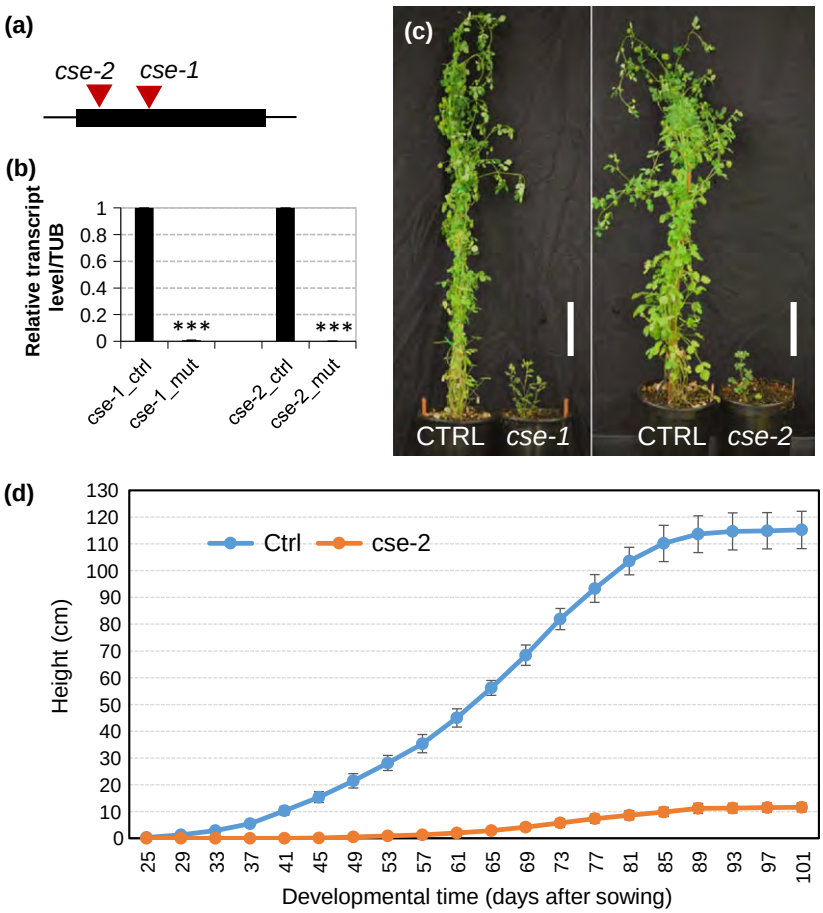

Figure 4. Identification and developmental phenotypes of *cse* mutants in *M. truncatula*.
(a) Diagram showing the position of the Tnt1 insertions in the *MtCSE* gene.
(b) Quantitative-PCR analysis of *MtCSE* transcripts. Data are means ± standard deviation (SD) ($n = 3$). ***$P < 0.001$, Student's *t*-test.
(c) Fully grown plants grown in long-day light condition for 3 months. Scale bar = 10 mm.
(d) Plant growth curve. Plant (inflorescence) height was measured every 4 days. The *Mtcse* mutation results in a dwarf plant with delayed growth. Ctrl represents plants with normal stature in segregating lines. $N = 20$ (controls) and 35 (*Mtcse* mutant).

Table 1 Developmental differences between *Atcse* and *Mtcse* plants

Plant	Genotype	Number of plants	Bolting time		Flowering time	
			Control	Mutant	Control	Mutant
A. thaliana	*Atcse-2*	32	17.5 ± 1.4	17.1 ± 1.3	23.5 ± 1.9	22.5 ± 1.3
M. truncatula	*Mtcse*-1	13	23.4 ± 2.5	43.3 ± 4.5***	54.9 ± 1.9	80.0 ± 4.4***
M. truncatula	*Mtcse*-2	14	24.1 ± 2.3	24.1 ± 2.3	55.1 ± 2.4	81.3 ± 3.8***

Data are means ± standard deviation (SD). ***$P < 0.001$, Student's *t*-test.

removal of soluble phenolics, no difference in UV autofluorescence, and loss of some Wiesner staining between cell files (compare Figure S5f–j with Figure 5f–j). However, there were still regions with very intense Wiesner staining (compare Figure S5d and Figure S5i). Taken together, these results suggest that soluble phenolic materials contribute to some, but not all, of the dark colour seen on Wiesner staining of *Mtcse* mutant stems.

Stem cross-sections were also examined by Mäule staining, a method in which S units are specifically stained a red colour (Lewis and Yamamoto, 1990). Mäule staining of control stems gave a typical strong red colour, whereas mutant stems showed decreased staining (Figure 5e,j), implying that the mutant stems had decreased S lignin content.

Lignin composition in *Mtcse* mutants

To quantitatively determine lignin composition, we analyzed lignin from wild-type and mutant stems using thioacidolysis. Analysis of thioacidolysis monomeric breakdown products by GC-MS indicated that the total thioacidolysis yield in *Mtcse* mutant stems was strongly decreased compared with that of control stems (Figure 6a). Levels of H-derived monomers were drastically increased in mutant compared to control stems (Figure 6b). In contrast, guaiacyl (G) monomers were highly decreased in

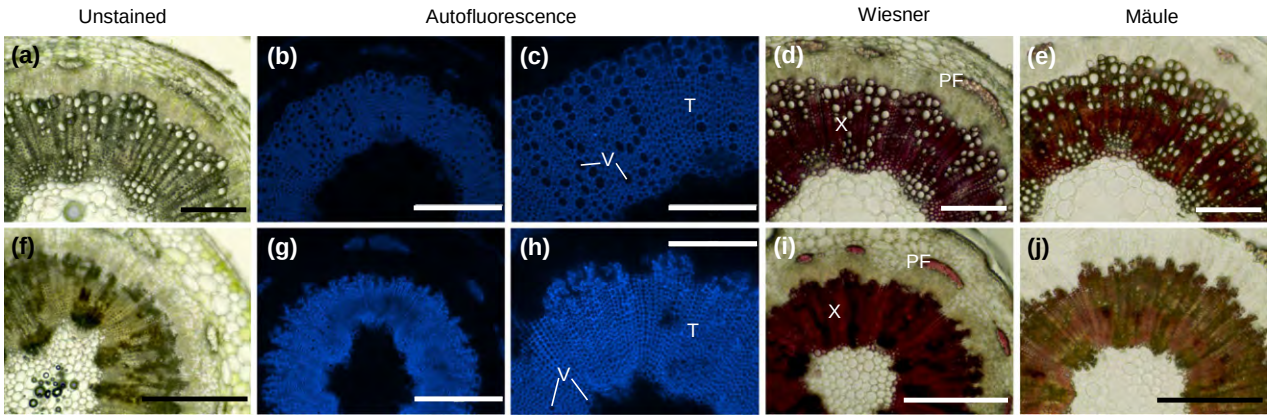

Figure 5. Histological analysis of *cse* mutant stems in *M. truncatula*.
(a–e) Control (ctrl) plant.
(f–j) *cse* mutant plant.
(a, f) Sectioned image without staining.
(b, c, g, h) UV autofluorescence of cross-section of the second internode. The blue colour is lignin autofluorescence in vascular bundles and interfascicular fibres.
(d, i) Wiesner (phloroglucinol) staining of cross-section of the second internode.
(e, j) Mäule staining of cross-section of the second internode.
Scale bars: 400 μm (a, b, d–g, i, j); 200 μm (c, h). PF, phloem fibre; T, tracheid; V, vessel element; X, xylem.

mutant stems and syringyl (S) monomers were modestly decreased, resulting in a significantly increased lignin S/G ratio in the mutant compared with the control (Figure 6d).

Nuclear magnetic resonance (NMR) analysis of *Medicago* cell walls

To complement the thioacidolysis analysis of lignin composition, and to further interrogate lignin structure in the *Mtcse* mutant, we performed whole-cell-wall gel-state NMR analysis. NMR assignments were based on previous studies (Kim and Ralph, 2010, 2014) and also by spectral comparison with synthetic H unit-derived lignins analyzed under the same NMR conditions. In the aromatic regions of the heteronuclear single-quantum correlation (HSQC) spectra of cell walls from the *Mtcse* mutant, dominant signals appeared from the H units derived from the normally minor monolignol *p*-coumaryl alcohol (Figure 7). The H units accounted for 76.6 and 84.0% of the total monomers in two independent *Mtcse* alleles, compared with 5.4–6.2% in three control lines (Figure 7). These data mirror the results of the thioacidolysis analysis (Figure 6b), which determines relative levels only from the fraction of β-*O*-4-linked units released as monomers. Analysis of the lignin aliphatic regions indicated that there were not major differences in the percentages of lignin linkage types between the wild-type and mutant plants (Figure S6), other than a decrease in the proportion of β-5 linkages in the mutant. This result is mildly surprising as the H-rich lignins in the ref8 (c3′h) single and med5a/5b ref8 triple Arabidopsis mutants displayed much more striking differences in inter-unit linkages compared with the lignin of the control plants (Ralph *et al.*, 2006; Weng *et al.*, 2010; Bonawitz *et al.*, 2014).

DISCUSSION

Genes encoding class I CSE enzymes are present in both dicots and monocots, but clearly not in all species. Furthermore, we were only able to detect weak esterase activity in extracts from stems of *B. distachyon* and corn, the genomes of which are among the 12 out of 61 species we examined by phylogenetic analysis that do not possess a class I *CSE* gene. The species that lacked a class I CSE gene, based on currently available sequence data, were *Brachypodium distachyon*, *Zea mays*, *Setaria italica*, *Sorghum bicolor*, *Oryza minuta*, *Aegilops tauschii*, *Hordeum vulgare* subsp. *vulgare*, *Erythranthe guttata*, *Beta vulgaris* subsp. *vulgaris*, *Ricinus communis*, *Gossypium raimondii*, and *Physcomitrella patens*. It was previously reported that there is no CSE enzyme activity in poplar (developing xylem), switchgrass (stems) and rice (Wang *et al.*, 2014). However, in our hands, crude switchgrass extracts had high CSE activity. Although it is possible that the presence of inhibitors resulted in an artefactual loss of CSE activity in *Brachypodium* and corn extracts, this seems unlikely given the high activity of CSE in switchgrass extracts prepared and assayed in the same way. Furthermore, although we have not examined developing xylem of *P. trichocarpa*, we observed high enzyme activity of recombinant CSE protein from another poplar species (*P. deltoides*, which possesses two CSEs that each exhibit 98% amino acid identity to their orthologs from *P. trichocarpa*). The *P. trichocarpa* CSEs are highly expressed in

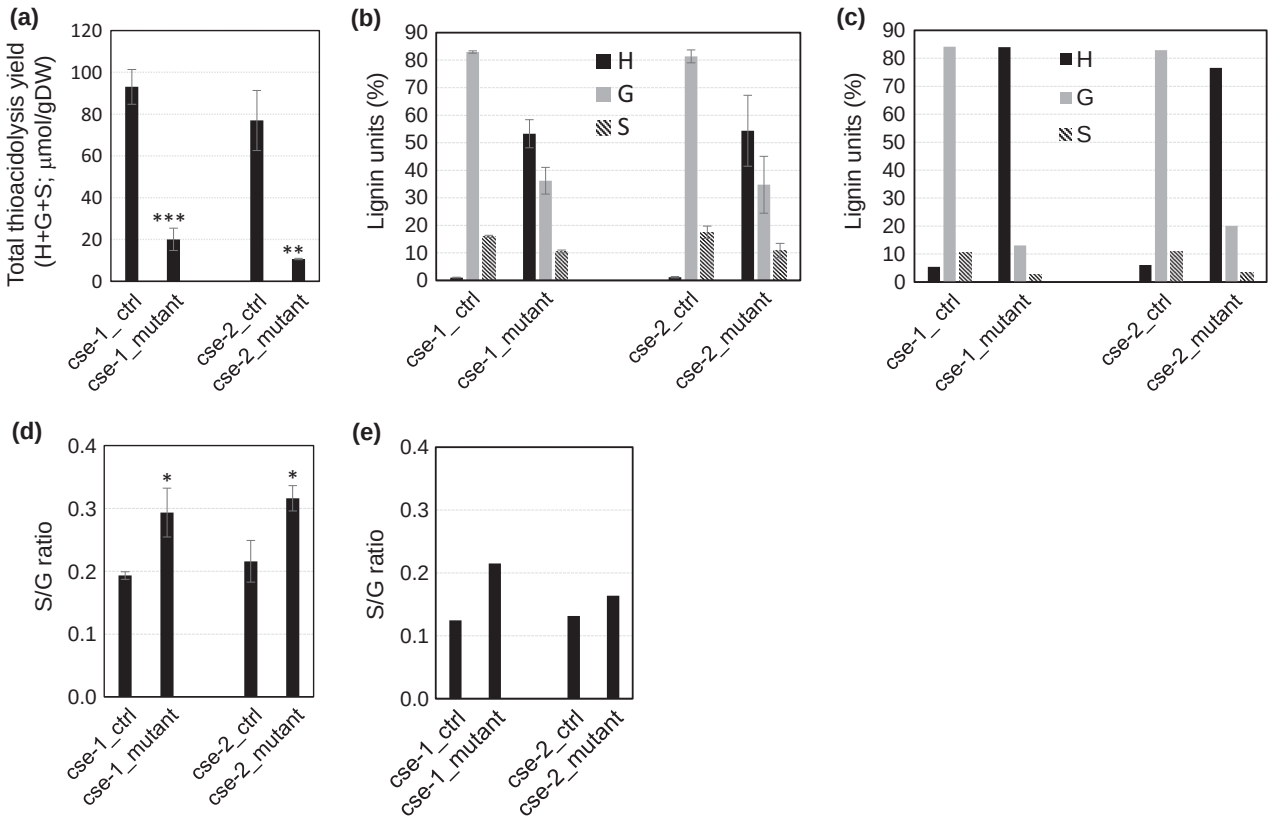

Figure 6. Lignin content and composition of stems of *cse* mutants and corresponding controls as determined by thioacidolysis and NMR.
(a) Total lignin determined by thioacidolysis yield. Data are means ± standard deviation (SD) ($n = 3$). ***$P < 0.001$, **$0.01 < P < 0.001$, Student's *t*-test.
(b, c) Lignin composition determined by thioacidolysis (b) and NMR analysis (c).
(d, e) S/G ratio determined by thioacidolysis (d) and NMR analysis (e). Data are means ± SD ($n = 3$). *$0.01 < P < 0.05$, Student's *t*-test.
Ctrl represents plants with normal plant phenotype in segregating lines.
H, hydroxyphenyl units; G, guaiacyl units; S, syringyl units.

stem tissues (PtCSE1_https://phytozome.jgi.doe.gov/pz/portal.html#!gene?search=1&crown=1&detail=1&method=0&searchText=transcriptid:26998824), so it seems counter-intuitive that they would not be expressed in developing xylem along with the HCT that generates their substrate.

Incubation of caffeoyl shikimate with buffer alone, or with enzyme extracts with low CSE activity, resulted in the appearance of a new compound with lower retention time but identical UV spectrum to the initial substrate. Initially, we thought that this compound might be an additional ester of shikimate, formed either by trans-esterification (Petersen, 2015) or possibly through additional activity of HCT; this latter type of reaction has recently been reported for formation of dicaffeoyl quinate (Vanholme *et al.*, 2013a; Moglia *et al.*, 2014). However, MS analysis indicated that the compound could not be a dicaffeoyl ester, and, because it is formed in the absence of enzyme, it is probably an adduct formed by reaction with a component in the buffer.

It will be important to determine, for species such as corn and *B. distachyon* that appear to lack a class I CSE, whether the low esterase activity observed in crude extracts is specific and involved in lignification, and, if not, if there exists a different type of HCT that efficiently catalyzes the reverse trans-esterification reaction to generate caffeoyl CoA for conversion to monolignols. In the absence of a CSE or an HCT for formation of caffeoyl CoA, it is unclear how the shikimate shunt could move beyond ester formation to function in monolignol biosynthesis. In the case of switchgrass, which does possess CSE, the two HCT enzymes show preferences of approximately 20-fold for the forward reaction to form coumaroyl shikimate compared to the reverse reaction converting caffeoyl shikimate to caffeoyl CoA (Escamilla-Treviño *et al.*, 2014).

It is clear from analysis of the *cse* mutants in *M. truncatula* that CSE is absolutely critical for monolignol biosynthesis in this species. The loss-of-function phenotype is more severe than that observed in the corresponding loss-of-function mutants in Arabidopsis, where growth is reduced by approximately 40%, total lignin reduced by approximately 36%, and H units comprise approximately 35% of the total monolignol-derived units (Vanholme *et al.*, 2013b). In the *M. truncatula* mutants, plants were much

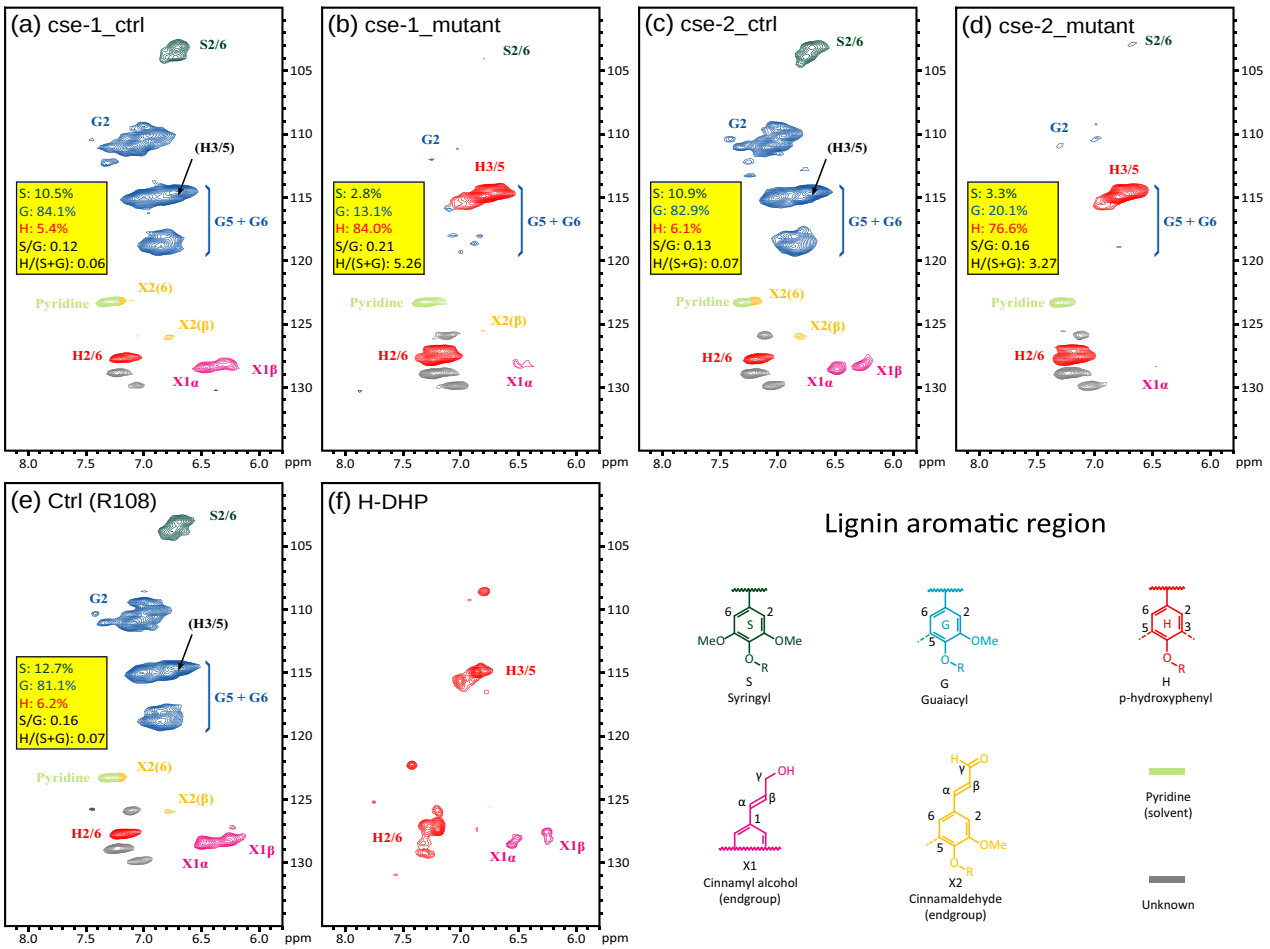

Figure 7. Analysis of *cse* mutant and wild-type cell walls of *M. truncatula* by NMR.
Partial HSQC spectra, showing aromatic regions, of ball-milled whole cell walls from *M. truncatula* and synthetic lignins (DHPs).
(a, c, e), Control plants (plants with normal plant phenotype in segregating lines).
(b, d) Mutant plants.
(f) Synthetic H lignin dehydrogenation polymer.

more severely stunted, total lignin was reduced by over 80%, and H units comprised approximately 50% of the monolignol-derived units as determined by thioacidolysis, and approximately 80% as determined by NMR. The difference between the thioacidolysis results and the values computed by NMR likely reflect the fact that some of the H units will not be present as β-*O*-4-linked units and therefore not released by thioacidolysis, and the over-estimation of the more mobile end-units in NMR (Tobimatsu *et al.*, 2013).

The difference in phenotype between the *Medicago* and Arabidopsis *cse* mutants could reflect differential abilities of HCT to catalyze the formation of caffeoyl CoA from caffeoyl shikimate in the two species. The kinetics of this reaction are not known in *Medicago*, but the reaction does occur in Arabidopsis and may therefore provide a means of by-passing the CSE reaction. HCT is, however, a critical enzyme in monolignol synthesis in *Medicago* species, at least in regard to the forward reaction; RNAi down-regulation of HCT to about 50% of wild-type activity in *M. sativa* (alfalfa) results in a 40% decrease in biomass, a 50% reduction in total lignin, and the appearance of H units to approximately 30% of total thioacidolysis-released monomers (Shadle *et al.*, 2007).

Although there was no difference in either bolting or flowing time in Arabidopsis *cse* mutants compared with control plants, *Mtcse* mutants showed highly delayed bolting and flowering time. This may reflect more severe impairment of vascular function in the *Mtcse* mutants.

As is typical in dicots, wild-type *Medicago* lignin contains mainly G and S subunits, with only a minor H component. The aromatic regions of the 2D HSQC spectra of cell walls from the *Medicago cse* mutant showed that the lignin comprises up to 85% of H units, which is very close to

the value recently reported in an Arabidopsis mutant (*med5a/b ref8-1*) in which the poor growth due to loss of function of coumaroyl shikimate 3′-hydroxylase is restored by loss of function of components of the Mediator complex (Bonawitz *et al.*, 2014). The H-subunit peak assignments in the aromatic region of spectra from the *Medicago* cse mutant were also confirmed by comparison with the peak patterns from an H-only synthetic lignin (dehydrogenation polymer, DHP) synthesized *in vitro* from *p*-coumaryl alcohol. The lignin interunit linkage distribution can normally be profiled easily in the aliphatic region, but the typical peaks are only found at trace level in the whole-cell-wall NMR data of the *cse* mutant samples, confirming the lower lignin contents in the mutants compared to those in the WT controls. The interunit ratios were only consistently changed in the *Medicago cse* mutant for β-*O*-5 linkages, differing from observations in previous studies of high-H lignins, in which C3H deficient Arabidopsis mutants showed a large difference in interunit linkage compared with control plants (Ralph *et al.*, 2006; Weng *et al.*, 2010; Bonawitz *et al.*, 2014).

The revisions to the lignin pathway that led to the acceptance of the shikimate shunt (Humphreys and Chapple, 2002; Hoffmann *et al.*, 2004), and the demonstration that ferulic acid (4-hydroxy,3-methoxy-cinnamic acid) arises from the oxidation of coniferaldehyde, at least in Arabidopsis (Nair *et al.*, 2004), suggested that free hydroxycinnamic acids are not intermediates in monolignol biosynthesis. The present results confirm the finding that, because of the action of CSE, free caffeic acid can be an intermediate in monolignol biosynthesis, but suggest that this may not be the case throughout the plant kingdom. In fact, it remains to be determined whether the shikimate shunt is conserved in all plant species. Although HCT down-regulation has been shown to reduce flux into lignin biosynthesis in several dicot species, the situation is less clear in monocots (Shen *et al.*, 2013). Further genetic analysis is necessary to resolve this issue, and *B. distachyon* will be a useful model because of its lack of a class I CSE.

EXPERIMENTAL PROCEDURES

Plant materials

Tobacco (*Nicotiana tabacum*) Tnt1 retrotransposon tagged mutants of *M. truncatula* (Tadege *et al.*, 2008) were screened to find *Mtcse* mutant plants. To confirm insertion lines, genotyping was conducted by using Tnt1-specific primers and *MtCSE* gene-specific primers (Table S1). The *Atcse-2* mutant (Salk_023077) was obtained from the ABRC at Ohio State University, USA and genotyping was carried out using T-DNA-specific primer and *AtCSE* gene-specific primers (Table S1).

Isolation of the *MtCSE* gene

In order to obtain the *MtCSE* sequence, the protein sequence of AtCSE (At1g52760) was used as a query for BLAST (BLASTP) analysis in the *Medicago* genome database at the J. Craig Venter Institute web site (http://blast.jcvi.org/er-blast/index.cgi?project=mtbe).

Plant growth conditions

Seeds were scarified with concentrated sulphuric acid for 7 min and then washed four times with distilled water. Scarified seeds were sterilized with 30% bleach for 4 min and then rinsed three times with sterile water. Sterilized seeds were vernalized at 4°C for 5 days and germinated for 5 days on half-strength B5 medium before transferring into soil. The *M. truncatula* plants were grown in a growth chamber set at 16 h/8 h day/night cycle at 22°C (day)/20°C (night), photoperiod (120 μm m^{-2} sec^{-1}) and 70–80% relative humidity.

Poplar (*P. deltoides*), *Zea mays* and *B. distachyon* were grown in the greenhouse at 24°C (day)/18°C (night). Switchgrass was grown in a growth chamber set at 16 h/8 h (day/night) cycle at 24°C (day)/18°C (night), photoperiod (140 μm m^{-2} sec^{-1}) and 50–60% relative humidity. *Arabidopsis thaliana* plants were grown in a growth chamber set at 16 h/8 h (day/night) cycles at 22°C (day)/20°C (night), photoperiod (150 μm m^{-2} sec^{-1}) and with 70–80% relative humidity.

Phylogenetic analysis

Multiple protein sequence alignments were performed using the ClustalW alignment tool. The phylogenetic tree was constructed using MEGA 6 (Tamura *et al.*, 2013). Node support was estimated using neighbor-joining bootstrap analysis (1000 bootstrap replicates). The protein sequence of AtCSE (At1g52760) was used as a query to BLAST (BLASTP) against the non-redundant protein sequence database of NCBI. Sequences from switchgrass were obtained from Phytozome v10.2 (http://phytozome.jgi.doe.gov/pz/portal.html). For obtaining CSE sequences from *P. deltoides*, PdCSE1 and PdCSE2 cDNAs were amplified by RT-PCR using forward and reverse primer pairs (Table S1) with SuperScript III reverse transcriptase (Invitrogen, Carlsbad, CA, USA), and confirmed by sequencing by Eurofins (Louisville, KY, USA).

Expression of poplar and *Medicago* CSEs in *E. coli*

Young developing internode tissue from stems of *P. deltoides* and *M. truncatula* were harvested and used for isolation of RNA with PureLink Plant RNA Reagent (Invitrogen, www.thermofisher.com). PdCSE1, PdCSE2 and MtCSE cDNAs were amplified by RT-PCR using forward and reverse primer pairs (Table S1) with SuperScript III reverse transcriptase (Invitrogen). Each cDNA was cloned into pCR8/GW/TOPO TA (Invitrogen) and then cloned into pDEST™17 Vector (Thermofisher Scientific, www.thermofisher.com, Waltham, MA, USA) by LR recombination reaction.

E. coli Rosetta strain cells harbouring the target CSE constructs were cultured at 37°C until OD600 reached 0.6–0.9, and isopropyl β-D-1-thiogalactopyranoside (IPTG) was then added to a final concentration of 0.5 mM to induce the heterologous protein expression. The culture was incubated at 18°C for 18–20 h, and tubes with 25 mL of culture were spun down to collect the pellets which were frozen at −20°C. Pellets were thawed, resuspended in 2 mL of extraction-washing buffer (10 mM imidazole, 50 mM Tris–HCl pH 8.0, 500 mM NaCl, 10% glycerol and 10 mM β-mercaptoethanol) and sonicated four times for 20 sec. The supernatants were recovered after centrifugation (16 000 ***g***), and equilibrated. Ni-NTA beads (Qiagen, www.qiagen.com) were added to allow the His-tagged proteins to bind to the beads. The suspension was incubated at 4°C for 30 min under constant inversion and unbound proteins were washed away three times with 1 mL of extraction-washing buffer. Target proteins were eluted with 400 μL of elution

solution (300 mM imidazole, 50 mM Tris–HCl buffer pH 7.5, 500 mM NaCl, 10% glycerol and 10 mM β-mercaptoethanol). Protein concentrations were determined using the Bio-Rad protein assay (Bio-Rad, www.bio-rad.com, Hercules, CA, USA).

Preparation of crude stem protein extracts

Young stem tissue from Brachypodium, switchgrass and corn (0.3–0.5 g) was ground very finely using a freezer mill (Retsch MM 400, www.retsch.com, Newtown, PA, USA), and crude protein extracts prepared as described previously (Gallego-Giraldo *et al.*, 2011).

Assay of CSE enzyme activity

Purified preparations of recombinant PdCSE1, PdCSE2 or MtCSE proteins (1–2 μg) and crude protein extracts of *Brachypodium*, corn and switchgrass (10 μg protein), were incubated at 30°C for 4 h with 100 mM NaPO4 buffer pH 7.5, 500 μM dithiothreitol and 100 μM caffeoyl shikimate in a final volume of 100 μL. Controls were made by stopping the above reactions before incubation or incubating with enzyme that had been pre-incubated at 95°C for 5 min, and spectra of authentic caffeic acid and caffeoyl shikimate standards were obtained using a 111 μM solution of these substrates. The reactions (including controls) were terminated by adding 10 μL of glacial acetic acid. Reaction products were injected onto an HPLC with a reverse-phase C18 column (Spherisorb 5μ ODS2, www.waters.com) and separated in a step gradient using 1% phosphoric acid in water as solvent A and acetonitrile as solvent B.

Liquid chromatography–mass spectrometry (LC–MS) analysis

LC–MS analyses were performed on an Agilent 1260 HPLC system coupled with Agilent 6400 Series Triple Quad LC/MS; the samples were injected onto a Waters Xterra MS C18 5 μm 250 × 2.1 mm column at a flow rate of 0.45 mL/min. Elution was carried out using mixtures of two solvents: A (0.1% formic acid in water) and B (0.1% formic acid in acetonitrile). The elution gradient was as follows: 0–2 min isocratic at 5% A, 5–27 min linear gradient from 5 to 45% of B, 27–28 min linear gradient up to 95% of B, 28–36 min isocratic at 95% of B, 36–37 min linear gradient from 95 to 5% B. MS scan was in negative mode. Mass range 100–1000; fragmentor voltage 135; gas temperature 350°C; gas flow 11 L min^{-1}; nebulizer 35 psi; sheath gas temperature 350°C; sheath gas flow 11 L min^{-1}; and capillary voltage negative 3500.

RNA isolation and real-time PCR

RNA from stems of *M. truncatula* was isolated using Plant RNA Reagent (Invitrogen, www.thermofisher.com). Isolated RNAs were treated with DNase I and then purified using an RNeasy MinElute Cleanup Kit (Qiagen, www.qiagen.com, Valencia, CA, USA). Cleaned rRNAs were used for reverse transcription with SuperScript III reverse transcriptase (Invitrogen). Quantitative real-time PCR (qRT-PCR) analysis with Power SYBR Green PCR Master Mix (Life Technologies, www.thermofisher.com) using primers surrounding the insertion site (Table S1) was performed on a QuantStudio 6 Flex Real-Time PCR system (Life Technologies) according to the manufacturer's instructions. Transcript levels were determined by relative quantification using *M. truncatula* β-*tublin* as a reference.

Histochemical analysis

The second internodes from fully grown but still green *M. truncatula* stems were cut and embedded in 7% agarose. Slices (100 μm thickness) were cut with a Vibratome (Microm HM650V, Thermo Scientific, www.thermofisher.com and Mäule stained as previously reported (Rohde *et al.*, 2004) with slight modifications: samples were prepared by incubating for 5 min in 1% KMnO4 (w/v), then rinsed with water, followed by incubation in 12% HCl (v/v) and observed after addition of a few drop of 1.5% $NaHCO_3$ (w/v). Images were taken with an AMG-EVOS microscope (AMEX-1200, Thermo Scientific). The images showing lignin UV autofluorescence were taken with an AMG-EVOS microscope (AMEX-4304, Thermo Scientific).

Removal of soluble phenolics from stem sections

Second internode tissues from *M. truncatula* were cut into approximately 5–6 mm lengths. The sections were incubated in sequence with the following solutions for 1 h with gentle shaking at room temperature, with the free liquid being removed after each incubation: 1 mL of 100% methanol (×2); 1 mL of chloroform/methanol (1:1, v/v) (×2); 1 mL of 100% methanol (×2); 1 mL of distilled water (×2). Treated internode tissue was then used for histological analysis as outlined above.

Determination of lignin content and composition

Whole stems excepting nodes were harvested. The collected samples were lyophilized and ground into powder. The lignin content and composition from stem material was determined by thioacidolysis (Lapierre *et al.*, 1985, 1995). Ten mg of extractive-free samples were incubated with 3 mL of a solution of 0.2 M BF3 etherate in an 8.75:1 dioxane/ethanethiol mixture. Lignin-derived monomers were identified by gas chromatography/mass spectrometry (GC/MS), and quantified by GC as their trimethylsilyl derivatives. GC/MS was performed on a Hewlett-Packard (Santa Clara, CA, USA) 7890A gas chromatograph equipped with an Agilent (Santa Clara, CA, USA) J&W column DB-5 ms (60 m × 0.25 mm × 0.25 μm film thickness) with a 5975C series mass selective detector. Mass spectra were recorded in electron impact mode (70 eV) with a 50–650 m/z scanning range.

Analysis of whole cell walls by NMR

Whole plant cell wall samples for gel-state NMR samples were prepared as previously described (Kim and Ralph, 2010; Mansfield *et al.*, 2012). The dried samples were pre-ground for 30 sec in a Retsch (Newtown, PA, USA) MM400 mixer mill at 30 Hz, using zirconium dioxide (ZrO2) vessels (10 mL) containing ZrO_2 ball bearings (2 × 10 mm). The cell walls were extracted with distilled water (ultrasonication, 1 h, three times) and 80% ethanol (ultrasonication, 1 h, three times). The cell walls were dried again and finely milled using a Fritsch planetary micromill PULVERISETTE 7 (Cranberry Township, PA, USA) at 600 rpm with ZrO_2 vessels (20 mL) containing ZrO_2 balls (10 mm × 10). Each sample (100 mg) was ground for 1 h 40 min (interval: 10 min, break: 5 min, repeated ×7). The cell walls were collected directly into the NMR tubes (50 mg for each sample) and gels formed using 0.5 mL dimethyl sulphoxide (DMSO)-d6/pyridine-d5 (4:1). NMR experiments were performed as previously described (Kim *et al.*, 2008; Kim and Ralph, 2010, 2014). NMR spectra were acquired on a Bruker Biospin (Billerica, MA, USA) Avance 700 MHz spectrometer equipped with a cryogenically cooled 5-mm TCI gradient probe with inverse geometry (proton coils closest to the sample). The central DMSO solvent peak was used as internal reference (δC 39.5, δH 2.49 ppm). The 1H–13C correlation experiment was an adiabatic HSQC experiment (Bruker standard pulse sequence 'hsqcetgpsisp.2'; phase-sensitive gradient-edited-2D HSQC using adiabatic pulses for inversion and refocusing) (Kupče and Freeman, 2007). HSQC experiments were carried out using the following parameters: acquired

from 11.5 to −0.5 ppm in F2 (1H) with 1682 data points (acquisition time 100 msec), 215 to −5 ppm in F1 (13C) with 620 increments (F1 acquisition time 8 msec) of 48 scans with a 500 msec interscan delay; the d24 delay was set to 0.86 msec (1/8J, J = 145 Hz). The total acquisition time was 5 h. Processing used typical matched Gaussian apodization (GB = 0.001, LB = −0.5) in F2 and squared cosine-bell and one level of linear prediction (32 coefficients) in F1. Volume integration of contours was performed on HSQC data processed without linear prediction using Bruker's TopSpin 3.1 (Mac version) software.

ACKNOWLEDGEMENTS

We thank Dr Jaime Barros-Rios for help with the GC–MS analysis, Jiangqi Wen for screening of TNT1 insertion lines, and the ABRC at Ohio State University for providing the AtCSE SALK knock-out line. This work was supported by the US National Science Foundation Integrated Organismal Systems Grant No. 1139489, the BioEnergy Science Center (Oak Ridge National Laboratory, DOE Office of Science BER DE-AC05-00OR22725) and the DOE Great Lakes Bioenergy Research Center (DOE Office of Science BER DE-FC02-07ER64494). The BioEnergy Science Center and Great Lakes Bioenergy Research Center are U.S. Department of Energy Bioenergy Research Centers supported by the Office of Biological and Environmental Research in the DOE Office of Science.

SUPPORTING INFORMATION

Additional Supporting Information may be found in the online version of this article.

Figure S1. Protein sequence alignment of CSEs.

Figure S2. LC-MS analysis of the products of CSE reactions with recombinant enzymes and crude extracts.

Figure S3. Expression pattern of the *CSE* gene in *Medicago truncatula*.

Figure S4. Phenotypes of leaf and seed pods of the *Mtcse* mutant.

Figure S5. Histological analysis of stem cross-sections from control and *cse* mutant *M. truncatula* after removal of soluble metabolites with methanol.

Figure S6. Partial HSQC spectra, showing aliphatic regions, of ball-milled whole cell walls from *M. truncatula* and synthetic lignins (DHPs).

Table S1. Oligonucleotides used in this study

REFERENCES

Bonawitz, N.D., Kim, J.I., Tobimatsu, Y. *et al.* (2014) Disruption of Mediator rescues the stunted growth of a lignin-deficient Arabidopsis mutant. *Nature*, **509**, 376–380.

Escamilla-Treviño, L.L., Shen, H., Hernandez, T., Yin, Y., Xu, Y. and Dixon, R.A. (2014) Early lignin pathway enzymes and routes to chlorogenic acid in switchgrass (*Panicum virgatum* L.). *Plant Mol. Biol.* **84**, 565–576.

Franke, R., Humphreys, J.M., Hemm, M.R., Denault, J.W., Ruegger, M.O. and Chapple, C. (2002) The Arabidopsis *REF8* gene encodes the 3-hydroxylase of phenylpropanoid metabolism. *Plant J.* **30**, 33–45.

Gallego-Giraldo, L., Escamilla-Trevino, L., Jackson, L.A. and Dixon, R.A. (2011) Salicylic acid mediates the reduced growth of lignin down-regulated plants. *Proc. Natl Acad. Sci. USA*, **108**, 20814–20819.

Hoffmann, L., Besseau, S., Geoffroy, P., Ritzenthaler, C., Meyer, D., Lapierre, C., Pollet, B. and Legrand, M. (2004) Silencing of hydroxycinnamoyl-coenzyme A shikimate/quinate hydroxycinnamoyltransferase affects phenylpropanoid biosynthesis. *Plant Cell*, **16**, 1446–1465.

Humphreys, J.M. and Chapple, C. (2002) Rewriting the lignin roadmap. *Curr. Opin. Plant Biol.* **5**, 224–229.

Jones, L., Ennos, A.R. and Turner, S.R. (2001) Cloning and characterization of *irregular xylem 4 (irx4)*: a severely lignin-deficient mutant of Arabidopsis. *Plant J.* **26**, 205–216.

Kim, H. and Ralph, J. (2010) Solution-state 2D NMR of ball-milled plant cell wall gels in DMSO-d(6)/pyridine-d(5). *Org. Biomol. Chem.* **8**, 576–591.

Kim, H. and Ralph, J. (2014) A gel-state 2D-NMR method for plant cell wall profiling and analysis: a model study with the amorphous cellulose and xylan from ball-milled cotton linters. *RSC Adv.* **4**, 7549–7560.

Kim, H., Ralph, J. and Akiyama, T. (2008) Solution-state 2D NMR of ball-milled plant cell wall gels in DMSO-d6. *Bioenerg Res.* **1**, 56–66.

Kupče, E. and Freeman, R. (2007) Compensated adiabatic inversion pulses: Broadband INEPT and HSQC. *J. Magnetic Res.* **187**, 258–265.

Lapierre, C., Monties, B. and Rolando, C. (1985) Thioacidolysis of lignin: comparison with acidolysis. *J. Wood Chem. Technol.* **5**, 277–292.

Lapierre, C., Pollet, B. and Rolando, C. (1995) New insight into the molecular architecture of hardwood lignins by chemical degradative method. *Res. Chem. Intermed.* **21**, 397–412.

Lewis, N.G. and Yamamoto, E. (1990) Lignin: occurrence, biogenesis and biodegradation. *Annu. Rev. Plant Physiol. Plant Mol. Biol.* **41**, 455–496.

Li, X., Bonawitz, N.D., Weng, J.-K. and Chapple, C. (2010) The growth reduction associated with repressed lignin biosynthesis in *Arabidopsis thaliana* is independent of flavonoids. *Plant Cell*, **22**, 1620–1632.

Liu, C., Jun, J. and Dixon, R.A. (2014) MYB5 and MYB14 play pivotal roles in seed coat polymer biosynthesis in *Medicago truncatula*. *Plant Physiol.* **165**, 1424–1439.

Mansfield, S.D., Kim, H., Lu, F. and Ralph, J. (2012) Whole plant cell wall characterization using 2D-NMR. *Nat. Protocols*, **7**, 1579–1589.

Moglia, A., Lanteri, S., Comino, C., Hill, L., Knevitt, D., Cagliero, C., Rubiolo, P., Bornemann, S. and Martin, C. (2014) Dual catalytic activity of hydroxycinnamoyl-Coenzyme A quinate transferase from tomato allows it to moonlight in the synthesis of both mono- and dicaffeoylquinic acids. *Plant Physiol.* **166**, 1777–1787.

Nair, R.B., Bastress, K.L., Ruegger, M.O., Denault, J.W. and Chapple, C. (2004) The *Arabidopsis thaliana REDUCED EPIDERMAL FLUORESCENCE1* gene encodes an aldehyde dehydrogenase involved in ferulic acid and sinapic acid biosynthesis. *Plant Cell*, **16**, 544–554.

Naoumkina, M.A., Modolo, L.V., Huhman, D.V., Urbanczyk-Wochniak, E., Tang, Y., Sumner, L.W. and Dixon, R.A. (2010) Genomic and co-expression analyses predict genes involved in triterpene saponin biosynthesis in *Medicago truncatula*. *Plant Cell*, **22**, 850–866.

Petersen, M. (2015) Hydroxycinnamoyltransferases in plant metabolism. *Phytochem. Rev.* doi: 10.1007/s11101-015-9417-1.

Pomar, F., Merino, F. and Barcelo, A.R. (2002) *O*-4-Linked coniferyl and sinapyl aldehydes in lignifying cell walls are the main targets of the Wiesner (phloroglucinol-HCl) reaction. *Protoplasma*, **220**, 17–28.

Ralph, J., Akiyama, T., Kim, H., Lu, F., Schatz, P.F., Marita, J.M., Ralph, S.A., Reddy, M.S.S., Chen, F. and Dixon, R.A. (2006) Effects of coumarate 3-hydroxylase down-regulation on lignin structure. *J. Biol. Chem.* **281**, 8843–8853.

Rohde, A., Morreel, K., Ralph, J. *et al.* (2004) Molecular phenotyping of the *pal1* and *pal2* mutants of *Arabidopsis thaliana* reveals far-reaching consequences on phenylpropanoid, amino acid, and carbohydrate metabolism. *Plant Cell*, **16**, 2749–2771.

Shadle, G., Chen, F., Reddy, M.S.S., Jackson, L., Nakashima, J. and Dixon, R.A. (2007) Down-regulation of hydroxycinnamoyl CoA: shikimate hydroxy cinnamoyl transferase in transgenic alfalfa impacts lignification, development and forage quality. *Phytochemistry*, **68**, 1521–1529.

Shen, H., Hisano, H., Hardin, F. *et al.* (2013) A genomic approach to deciphering the monolignol pathway in switchgrass (*Panicum virgatum* L.). *Plant Cell* **25**, 4342–4361.

Tadege, M., Ratet, P. and Mysore, K.S. (2005) Insertional mutagenesis: a Swiss army knife for functional genomics of *Medicago truncatula*. *Trends Plant Sci.* **10**, 229–235.

Tadege, M., Wen, J., He, J. *et al.* (2008) Large scale insertional mutagenesis using *Tnt1* retrotransposon in the model legume *Medicago truncatula*. *Plant J.* **54**, 335–347.

Tamura, K., Stecher, G., Peterson, D., Filipski, A. and Kumar, S. (2013) MEGA6: molecular Evolutionary Genetics Analysis version 6.0. *Mol. Biol. Evol.* **30**, 2725–2729.

Thévenin, J., Pollet, B., Letarnec, B., Saulnier, L., Gissot, L., Maia-Grondard, A., Lapierre, C. and Jouanin, L. (2011) The simultaneous repression of CCR and CAD, two enzymes of the lignin biosynthetic pathway, results in sterility and dwarfism in *Arabidopsis thaliana*. *Mol. Plant*, **4**, 70–82.

Tobimatsu, Y., Chen, F., Nakashima, J., Jackson, L.A., Dixon, R.A. and Ralph, J. (2013) Coexistence but independent biosynthesis of catechyl and guaiacyl/syringyl lignin polymers in seed coats. *Plant Cell*, **25**, 2587–2600.

Vanholme, B., Cesarino, I., Goeminne, G. *et al.* (2013a) Breeding with rare defective alleles (BRDA): a natural *Populus nigra* HCT mutant with modified lignin as a case study. *New Phytol.* **198**, 765–776.

Vanholme, R., Cesarino, I., Rataj, K. *et al.* (2013b) Caffeoyl shikimate esterase (CSE) is an enzyme in the lignin biosynthetic pathway. *Science*, **341**, 1103–1106.

Wang, J.P., Naik, P.P., Chen, H.-C. *et al.* (2014) Complete proteomic-based enzyme reaction and inhibition kinetics reveal how monolignol biosynthetic enzyme families affect metabolic flux and lignin in *Populus trichocarpa*. *Plant Cell*, **26**, 894–914.

Weng, J.-K., Akiyama, T., Bonawitz, N.D., Li, X., Ralph, J. and Chapple, C. (2010) Convergent evolution of syringyl lignin biosynthesis via distinct pathways in the lycophyte Selaginella and flowering plants. *Plant Cell*, **22**, 1033–1045.

